RSC Advances

This is an *Accepted Manuscript*, which has been through the Royal Society of Chemistry peer review process and has been accepted for publication.

Accepted Manuscripts are published online shortly after acceptance, before technical editing, formatting and proof reading. Using this free service, authors can make their results available to the community, in citable form, before we publish the edited article. This *Accepted Manuscript* will be replaced by the edited, formatted and paginated article as soon as this is available.

You can find more information about *Accepted Manuscripts* in the Information for Authors.

Please note that technical editing may introduce minor changes to the text and/or graphics, which may alter content. The journal's standard Terms & Conditions and the Ethical guidelines still apply. In no event shall the Royal Society of Chemistry be held responsible for any errors or omissions in this *Accepted Manuscript* or any consequences arising from the use of any information it contains.

ROYAL SOCIETY OF CHEMISTRY

www.rsc.org/advances

Adsorption of Au_n (n = 1-4) clusters on Fe_3O_4(001) B-termination

Authors:

Xiaohu Yu,[a,b,*] Xuemei Zhang,[a] Shengguang Wang,[b,c] Gang Feng[b,d,e,*]

Affiliation:

[a] *College of Physics and Electrical Engineering, Anyang Normal University, Anyang, Henan, 455000, P.R. China*

[b] *State Key Laboratory of Coal Conversion, Institute of Coal Chemistry, Chinese Academy of Sciences, Taiyuan, Shanxi 030001, P.R. China*

[c] *China Synfuels China Co., Ltd., Huairou, Beijing 101407, P.R. China*

[d] *Shanghai Research Institute of Petrochemical Technology SINOPEC, 201208, Shanghai, P.R. China*

[e] *College of Chemistry, Nanchang University, Nanchang, Jiangxi 330031 P.R. China;*

Corresponding authors:

Xiaohu Yu Tel:+86 372 2900041; fax: +86 372 2900041; Email: yuxiaohu950203@126.com

Gang Feng Tel:+86 21 68462197; fax:+86 21 68462283; Email: fengg.sshy@sinopec.com

RSC Advances Accepted Manuscript

Abstract: For understanding the catalytic properties of Au nanoparticles supported on iron oxide, the adsorption structures and energies of Au_n (n = 1–4) clusters on the stoichiometric, reduced and hydrated Fe_3O_4(001) B-terminations were systematically studied by using GGA density functional theory method including the Hubbard parameter (U) to describe the on-site Coulomb interaction. It was found that the formation of reduced surface with oxygen vacancy is much easier than that of oxidized surface with iron vacancy. The most stable hydrated surface has dissociative H_2O adsorption with the formation of surface hydroxyls, in agreement with the recent computational and experimental studies. Different adsorption configurations of Au_n clusters have been found on the three surfaces. Au clusters prefers to bind with surface iron atoms, compared to surface oxygen atoms. The most stable adsorption configuration of single Au adatoms on the long bridge site to two surface O atoms is supported by the recent experimental study. The adsorbed Au atoms on surface iron atoms are reduced and negatively charged; and the Au atoms interacting either with surface oxygen atom or the surface hydroxyl have less negative or positive charge. The surface hydroxyls can stabilize the adsorption of Au_n clusters.

Keywords: Density functional theory, Fe_3O_4(001) B-termination, Au clusters, Surface hydroxyl, Catalysis

RSC Advances Accepted Manuscript

1. Introduction

Metallic gold supported on transition metal oxides has attracted intensive research interest[1-3] because of the excellent catalytic activity in promoting various reactions including low temperature CO oxidation[4] and water-gas shift (WGS) reaction.[5,6] As gold is chemically inert, it is surprising that supported gold can have catalytic activity.[7] The high catalytic activity of supported gold has been attributed to structure (size, shape and oxidation state) and support effects.[8,9] Iron oxide Fe_3O_4 is one of the mostly used support materials.[3,10] To understand the catalytic activity of Au/Fe_3O_4, detailed structure information of gold atoms on iron oxide is undoubtedly of theoretical and practical importance.[10,11]

In a scanning tunneling microscopy/scanning tunneling spectroscopy study of supported gold nanoparticles on a reduced $Fe_3O_4(111)$ surface in ultrahigh vacuum, Rim et al.[12] found that gold nanoparticles exhibit metallic electronic character and gold adatom is positively charged, and the key role of gold atom has been emphasized in CO oxidation and WGS reaction. Lee et al.[13] studied H_2O_2 reduction on individual Au/Fe_3O_4 nanoparticles and found experimentally that the enhanced catalytic activity arises from the polarization effect at the Au/Fe_3O_4 interface, where Fe_3O_4 becomes more active. It has been reported that oxidized Au species on Fe_3O_4 are active sites for low temperature WGS reaction,[14,15] while gold nanoparticles are spectators. Shaikhutdinov et al. [16] studied CO adsorption on gold model catalysts and found that CO adsorded on gold exhibits a size effect and small gold particles adsorb CO more strongly. Zhu et al.[17] reported that the positively charged gold atoms linked to the lattice oxygen of Fe_3O_4 have remarkably high activity in crotonaldehyde hydrogenation. Using scanning tunneling microscopy, X-ray photoemission spectroscopy and Mössbauer spectroscopy, in situ, under ultrahigh vacuum conditions, Spiridis et al.[18] studied the cluster-support interaction in a $Au/Fe_3O_4(001)$ system and found that Au nucleation process is done below a nominal coverage of 0.3 monolayer and the

RSC Advances Accepted Manuscript

three-dimensional growth mode is dominant at higher coverages. By using scanning tunneling microscopy, Jordan et al.[19] studied the interaction of Au on $Fe_3O_4(001)$ and found that the oxygen vacancy sites are the initial nucleation of Au cluster. Gatel et al. studied the epitaxial growths of Pt, Au and Ag on $Fe_3O_4(001)$[20] as well as Au and Pt on $Fe_3O_4(111)$[21] and found different growth modes upon deposition temperature and thickness. Recently, Parkinson et al. [22] studied gold deposition on $Fe_3O_4(001)$ at room temperature using scanning tunneling microscopy and X-ray photoelectron spectroscopy and found the surface forms a $(\sqrt{2}\times\sqrt{2})R45°$ reconstruction, where pairs of Fe and neighboring O ions are slightly displaced laterally producing undulating rows with narrow and wide hollow sites, which are the bicoordinated O_1 sites. At low coverages, single Au adatoms adsorb exclusively at the narrow sites, with no significant sintering at temperatures up to 400 °C, indicating its high thermal stability.

On Au nanocluster on TiO_2, Veith et al.[23] found that introducing surface hydroxyls results in at least a 180-fold increase in CO oxidation activity. Brown et al.[24,25] investigated the nucleation and electronic structure of vapor deposited gold on hydroxylated MgO(001) surfaces under ultrahigh vacuum condition and found that gold atoms interact with a specific type of hydroxyl groups, resulting in the formation of oxidized gold particles. They also found that the enhanced adhesion of Au particles, due to the formation of strong Au–O interfacial bonds, is responsible for the observed higher stability of small Au clusters toward thermal sintering on hydroxylated MgO surfaces. Jiang et al.[26] explored the interaction between gold nanoclusters and a fully hydroxylated surface, the basal plane of $Mg(OH)_2$, and found strong interaction between gold nanoclusters and the surface hydroxyls via a short bond between edge Au atoms and O atoms of the hydroxyls. Ganesh et al.[27] studied the role of hydroxyls on the catalytic activity of supported Au clusters on TiO_2 and found that hydroxyls have a long range effect increasing the adhesion of gold clusters and enhances the molecular adsorption.

RSC Advances Accepted Manuscript

Theoretically, our group studied the adsorption of alkali metals on the $Fe_3O_4(111)$ surface[28] by using density functional theory (DFT) method and found that Li atom has the strongest adsorption energy. Recently, we studied single Au atom adsorption on the six terminations of the $Fe_3O_4(111)$ surface using GGA+U method, and found correlation between the surface stability and the Au atom adsorption energy for the most stable adsorption configurations, i.e.; the more stable the surface, the lower the Au atom adsorption energy, and it is also found that Au atom has negative charge on the iron terminated surfaces while positive charge on the oxygen terminated surface[29]. In addition, we systematically researched the late transition metal atom adsorption on the $Fe_3O_4(111)$ surface.[30] Using DFT+U, Kiejna et al.[31] studied the adsorption of Au and Pd atoms on $Fe_3O_4(111)$ and found that the adsorption of Au and Pd on oxygen terminated surface is stronger than on iron terminated surface.

Since single Au atom is too simple to represent Au nanoparticles, we studied the adsorption of small Au clusters on the Fe_3O_4 surface for the understanding of the catalytic activity of Au/Fe_3O_4 systems in CO oxidation and water-gas shift reaction at the DFT level under the consideration of the on-site Coulomb interaction (GGA+*U*) method. This is the first paper dealing with the adsorption of small Au clusters, Au_n (n=1–4), on the stoichiometric, reduced (with oxygen vacancy) and hydrated $Fe_3O_4(001)$ surfaces.

2. Method and Surface Model

2.1 Method

The full spin-polarized calculations were performed by using the frozen-core all-electron projector-augmented wave (PAW) method,[32] as implemented in Vienna ab initio simulation program (VASP).[33-35] The 3*p*, 4*s* and 3*d* electrons of Fe, the 2*s* and 2*p* electrons of O and the 5*d* and 6*s* electrons of Au were treated as valence electrons. The electron exchange and correlation were treated within the generalized gradient approximation using the Perdew-Burke-Ernzerhof

RSC Advances Accepted Manuscript

(GGA-PBE) functional.[36] In addition, the strong on-site Coulomb corrections are included, since it can accurately model transition metal oxide systems.[37,38] The physical insight of GGA+*U* comes from the Hubbard Hamiltonian, in which the Hubbard parameter (*U*) is introduced for Fe *3d* electrons to describe the on-site Coulomb interaction. The value of $U_{eff} = U\text{-}J$ was set to 3.8 eV as suggested in literatures.[39-41] At U_{eff} = 3.8 eV, the computed magnetic moments of the tetrahedral and octahedral iron sites are 4.0 μ_B, in well agreement with the experiment (4.05 μ_B).[42,43] The number of plane waves was controlled by a cutoff energy of 400 eV. The Brillouin-zone integrations were performed using Monkhorst-Pack (MP) grids[44] and a Gaussian smearing of = 0.2 eV. For integration within the Brillouin zone, a MP grid of 3×3×1 was used for Fe_3O_4(001). The structure optimization was performed as the force on each atom was less than 0.02 eV/Å. These settings are able to generate lattice constants of 8.405 Å for bulk Fe_3O_4, in close to the experimental values 8.396 Å, [42] and to reproduce the characteristic electronic features including the energy level of *d* states and the half-metal solution of Fe_3O_4. There are two distinct Fe cation sites: tetrahedral *A* sites and octahedral *B* sites. In an ionic picture, the tetrahedral *A* sites are occupied by Fe^{3+}, the octahedral *B* sites are occupied by an equal number of Fe^{2+} and Fe^{3+}. We set spin up for octahedral Fe and spin down for tetrahedral Fe because ferrimagnetic Fe_3O_4 is preferred than ferromagnetic state.[45,46]

2.2 Surface Model

The Fe_3O_4(001) surface can be viewed as a stacking sequence of two alternating layers; the A-layer has Fe^{3+} in tetrahedral coordination, and the B-layer has rows of Fe^{2+} and Fe^{3+} in octahedral coordination. The Fe_3O_4(001) ($\sqrt{2}\times\sqrt{2}$) B termination was chosen as substrate since it is indicative from quantitative X-ray diffraction,[47] LEED analyses,[48] STM[49] and DFT calculations. [42,50] We have modeled the Fe_3O_4(001) B-termination with an 8-atomic-layer slab by truncating the bulk Fe_3O_4 structure as shown in Fig. 1. The B-termination is represented as slabs, repeated

RSC Advances Accepted Manuscript

periodically in z direction perpendicular to the surface and separated from their images by 16 Å vacuum gaps, which have been found thick enough for single Au atom adsorption on the Fe_3O_4(111) surface.[29] The dimensions of x and y of the unit cell are fixed at the calculated equilibrium lattice parameter value (8.405 Å). For structure optimization, the top four layers and the adsorbed Au clusters are fully relaxed and the bottom four layers are fixed. The leading errors induced by the existence of dipole moment in the supercells were corrected by using the methods as implemented in the VASP code. [33]

(Fig. 1)

We present the results of Au_n clusters (n = 1-4) on the stoichiometric Fe_3O_4(001) B-terminated surface and the surface with an oxygen vacancy as well as the hydrated surface with one H_2O molecule. In Fe_3O_4(001) B-termination, iron cations occupy the tetrahedral (Fe_A) and octahedral (Fe_B) sites, and each oxygen atom has four Fe–O bonds (one Fe_A–O and three Fe_B–O bonds). To facilitate the characterization, we used the following notions for the possible adsorption sites in Fig. 1; the top sites of **O_1** (three O-Fe_B bonds) and **O_2** (two O-Fe_B and one O-Fe_A bonds), **Fe_1** (surface octahedral iron Fe_B) and **Fe_2** (second layer tetrahedral iron Fe_A) as well as the bridge sites of **bri_1** (the bridge site of O_1-O_1), **bri_2** (the bridge site of O_2-O_2) and bri_3 (the long bridge site of O_1–O_1).

The adsorption energy (E_{ads}) is used to characterize the interaction strength of Au atoms on the surface,[51] $E_{ads} = E(Au_n/Fe_3O_4) - [E(Au_n) + E(Fe_3O_4)]$, where the $E(Au_n/Fe_3O_4)$, $E(Fe_3O_4)$ and $E(Au_n)$ are the energies of the adsorbed Au_n cluster on Fe_3O_4 (Au_n/Fe_3O_4), the Fe_3O_4 slab (clean, reduced and hydrated surface, respectively), and the most stable Au_n cluster, respectively. A negative E_{ads} indicates a stabilizing interaction.

3. Results and discussion

3.1 Au_n clusters

RSC Advances Accepted Manuscript

There are many works investigated the gas phase structures of Au_n clusters, and the results depend on the methods.[52-59] In our study we are only interested in Au_n (n = 1-4) clusters (Fig. 2) for adsorption. For Au_2, the computed binding energy (–2.28 eV) is close to the reported experimental value (–2.47 eV).[60] For Au_3, the triangular and the linear structures are nearly degenerated (0.01 eV). For Au_4, the rhombus and T-shape structures are nearly degenerated (0.01 eV), and the tetrahedral isomer is 1.21 eV less stable.

(Fig. 2)

3.2 Au_n on Fe_3O_4(001) B-termination

In this paper, we mainly consider the effect of different Fe_3O_4(001) surfaces on Au_n (n = 1-4) clusters adsorption. It should be noted that Au_n (n = 1-4) clusters are not the perfect model to describe all gold nanoparticles in various catalysts. While, how to make a good model to represent Au nanoparticles is not in the scope of this paper. All possible sites and adsorption configurations for Au_n (n = 1-4) adsorption are considered in the present work, and all optimized configurations are shown in Supporting Information Fig. S1-12. The most stable configurations are shown in Fig. 3. Since the stoichiometric Fe_3O_4(001) B-termination has eight oxygen atoms and four octahedral iron atoms, the largest gold concentration is 33.3% for Au_4 adsorption.

(Fig. 3)

For Au_1, the most stable configuration has Au atom at the long bridge site of two O_1 atoms with adsorption energy of –3.44 eV (Fig. 3-a1), and the Au-O_1 distances are 1.997 and 2.014 Å. For Au_2, the stable configuration has side-on Au adatom bridging two octahedral iron atoms with adsorption energy of –2.31 eV (Fig. 3-b1) and the Au-Fe distance is 2.607 Å. The distance of Au-Au in dimer is 2.527 Å which is shorter than binding on the Fe_3O_4(001) surface. For Au_3, various low-lying isomers of free Au_3 clusters were considered, and the most stable one has side-on adsorption of a triangle Au_3 on two octahedral iron atoms with adsorption energy of –2.27 eV

RSC Advances Accepted Manuscript

(Fig. 3-c1). For Au_4, many adsorption configurations have been considered; and they have irregular structural patterns, and the most stable one has three Au atoms interacting with two surface iron atoms and one surface oxygen atom (Fig. 3-d1), and the adsorption energy is –2.09 eV. It is to note that no stable adsorption configurations of Au atoms at the top of O_1 and O_2 or bridging two oxygen atoms have been found and free optimization led to the most stable adsorption configurations as discussed above.

To characterize the oxidation state of the adsorbed Au_n clusters, we performed Bader analysis to get the charge transfer between the clusters and support (Fig. 3-a1-d1). All Au atoms interacting with surface iron atoms have negative charge, indicating charge transfer from surface iron atoms to the adsorbed Au atoms and the reduction of the Au atoms by surface iron atoms. For Au_4 cluster, it also shows that the Au atom interacting with surface oxygen atom has positive charge, indicating the oxidation of the Au atom by surface oxygen atom. Such charge transfer between the surface atoms and the adsorbed Au atoms is associated with the electronegativity for Fe (1.83) atom, Au atom (1.92) and oxygen atom (3.61).[61] The totally transformed charge is +0.418 for Au_1; –0.291 for Au_2, –0.198 for Au_3 and +0.035 for Au_4.

3.3 Au_n on reduced Fe_3O_4(001) B-termination

In addition to the stoichiometric surface, we are interested in Au_n adsorption on the surface with vacancies. At first we computed the formation energy of surface oxygen vacancy[62] [E(O) = E(V) + E(O_2)/2 – E(slab)] and surface iron vacancy[63] [E(Fe) = E(V) + E(Fe/bulk) – E(slab)]; where E(V) is the total energy of the slab with oxygen or iron vacancy, E(slab) is the total energy of the slab, E(O_2) is the total energy of O_2 molecule, and E(Fe/bulk) is the energy of one Fe atom in bulk. The formation energy of the first and second oxygen vacancy is 1.11 and 3.43 eV, respectively; and the formation energy of iron vacancy is 3.03 eV. Thus the first oxygen vacancy can be formed much easier than the iron vacancy; and we only consider the Fe_3O_4(001) B-

RSC Advances Accepted Manuscript

termination with one oxygen vacancy, and the vacancy concentration is 8.3% on the basis of eight surface oxygen and four surface iron atoms. That the formation of the first oxygen vacancy is easier than that of the second oxygen vacancy is also reported by Mulakaluri et al.[64] With the formation of oxygen vacancy, the surface is reduced and becomes electron rich. Compared to the clean surface, two surface octahedral iron atoms near the oxygen vacancy is less positively charged by 0.39 e, indicating their formal reduction from Fe^{3+} to Fe^{2+}; and similar change is also found for the third layer octahedral iron atoms near the oxygen vacancy (less positively charged by 0.31 e). All possible adsorption sites for Au_n clusters on the reduced Fe_3O_4(001) B-termination are examined and the corresponding lowest energy structures are given in Fig. 2.

For Au_1 (Fig. 3-a2), the most stable configuration has Au atom on the oxygen vacancy and adsorption energy of –2.51 eV; and the Au–Fe distances are 2.660 and 2.636 Å; and Au atom initially put on surface iron and oxygen near the oxygen vacancy moves to the oxygen vacancy automatically. For Au_2 (Fig. 3-b2), the most stable configuration has adsorption energy of –2.50 eV; and the Au atom on the oxygen vacancy has distance of 2.109 Å to the neighboring O atom, while the second Au atom bridges two octahedral iron atoms with distances of 2.729 and 2.834 Å. For Au_3 (Fig. 3-c2), the most stable configuration has adsorption energy of –3.31 eV; and the Au atom on the oxygen vacancy has distance of 2.259 Å to the neighboring oxygen atom, and the other two Au atoms have distances of 2.586 and 2.672 Å to the octahedral iron atoms. Fig. 2-d2 shows the most stable Au_4 configuration with adsorption energy of –2.67 eV. The Au atom on the oxygen vacancy has distance of 2.288 Å to the neighboring oxygen atom; and the other three Au atoms adsorbed on three surface octahedral iron atoms have Au–Fe distances of 2.813, 2.730 and 2.665 Å, respectively.

Since the surface with oxygen vacancy is reduced and electron rich, and Au atom is more electronegative than Fe atom, it is to expect the charge transfer from the defect surface to the

RSC Advances Accepted Manuscript

adsorbed Au_n clusters, i.e.; all Au atoms interacting with surface iron atoms are reduced and have negative charge (Fig. 3-a2-d2); and the transformed charge is –0.429 for Au_1; –0.174 for Au_2, –0.510 for Au_3 and –0.468 for Au_4, similar as on the clean surface.

3.4 Au_n on the hydrated Fe_3O_4(001) B-termination

Since H_2O is available in the preparation of Fe_3O_4, we have calculated one H_2O molecule adsorption on the Fe_3O_4(001) B-termination. Since the Fe_3O_4(001) termination has four octahedral iron atoms, one H_2O adsorption corresponds to a surface concentration of 25 %. The H_2O adsorption energy is defined as $E(H_2O) = E(H_2O/slab) - [E(H_2O) - E(slab)]$, where $E(H_2O/slab)$ is the total energy of the slab with adsorbed H_2O, $E(slab)$ is the total energy of the slab, $E(H_2O)$ is the total energy of gas phase H_2O. For H_2O adsorption on the Fe_3O_4(001) B-termination, we have found molecular and dissociative adsorptions. For the molecular adsorption, the most stable configuration has only interaction between surface iron atom and the oxygen atom of H_2O with adsorption energy of –1.10 eV. For the dissociative adsorption, one hydrogen atom binds to surface O_1 to form O_1–H and the OH group binds to surface iron; and the adsorption energy is –1.21 eV. Our results are in agreement with the recent experimental studies of H_2O dissociative adsorption on Fe_3O_4(001) by Parkinson et al.[65] and also with the recent GGA+U studies of H_2O adsorption on Fe_3O_4(001) by Mulakaluri et al.[64] and their reported H_2O dissociative adsorption energy of –0.76 eV is smaller than our value of –1.21 eV.

For Au_n adsorption, we used the hydrated surface with two surface OH groups and the most stable configurations are shown in Fig. 3. For Au_1 (Fig. 3-a3), the most stable configuration with Au atom on the long bridge site of two surface O_1 atoms has adsorption energy of –3.16 eV, and the distances of Au–O_1 are 2.043 and 2.004 Å, respectively. For Au_2 (Fig. 3-b3), the most stable configuration has Au_2 on top of two surface irons with adsorption energy of –2.44 eV. One gold atom of Au_2 and O of OH form a O–Au bond with distance of 2.143 Å, the Au–Au distance is

RSC Advances Accepted Manuscript

2.564 Å. The two Au atoms form two Au-Fe bonds with distances of 2.676 and 2.810 Å. For Au_3 (Fig. 3-c3), the most stable configuration has Au_3 triangle vertically on the top of surface iron along the surface iron rows with adsorption energy of –2.89 eV. One Au atom of Au_3 bridges two surface iron atoms with distances of 2.647 and 2.801 Å, another Au atom of Au_3 interacts with the oxygen atom of OH with Au–O distance 2.100 Å. For Au_4 (Fig. 3-d3), the most stable configuration has deformed Y-shape of Au_4 with adsorption energy of –3.31 eV. One Au atom of Au_4 interacts with surface oxygen atom and has Au–O distance of 2.135 Å; and another Au atom interacts with surface hydroxyl O and has Au–O distance of 2.222 Å. The distances between Au atoms and surface iron atoms are 2.625 and 2.850 Å, respectively. We also calculated H spillover on single Au adsorption on hydrated surface and H spillover from bicoordinated O to hydroxyl is not favorable thermodynamically on the hydrated surface (Supporting Information Fig. S13).

Fig. 3 shows that the most stable Au_n adsorption configurations have direct interaction of Au atom with surface hydroxyl group; and Au atoms interacting with either surface hydroxyl or surface oxygen have less negative or positive charge, compared to that of the clean surface and the Au atoms on surface iron have negative charge. The transformed charge is +0.429 for Au_1; –0.017 for Au_2, +0.104 for Au_3 and –0.063 for Au_4 on the hydrated Fe_3O_4(001) surface.

3.5 Discussion

It is now interesting to compare Au_n adsorption on the stoichiometric, reduced and hydrated Fe_3O_4(001) B-terminations. It is found that the surface oxygen vacancy can be formed much easier than surface iron vacancy; and the surface with oxygen vacancy is reduced and becomes electron rich compared to the stoichiometric surface. For H_2O adsorption, dissociative adsorption is more favorable than the molecular adsorption and the dissociated H binds to surface oxygen and the OH group binds to surface iron atom.

In the same time, we consider that atomic Au adsorption on stoichiometric surface (supporting

RSC Advances Accepted Manuscript

information Fig. S14), for two Au atoms, the most stable configuration is that two Au atoms adsorbed on two bicoordinated O_1 sites respectively with adsorption energy of -3.23 eV. For three Au atoms, the most stable configuration is that two Au atoms adsorbed on the two bicoordinated O_1 sites and another gold atom adsorbed on top of one of octahedral iron with adsorption energy of -2.95 eV. For four Au atoms, the most stable configuration is that two Au atoms adsorbed on the two bicoordinated O_1 sites and other two gold atoms adsorbed on top of two octahedral iron atoms with adsorption energy of -2.95 eV. Comparing with the adsorption energies of Au_2 (-2.31 eV), Au_3 (-2.27 eV), Au_4 (-2.09 eV), we can clearly see that agglomeration of one more Au_n clusters is not favorable on stoichiometric $Fe_3O_4(001)$ surface. This is well agreement with recently experimental reports.[22] On reduced surface, the adsorption energies of two Au atoms, three Au atoms and four Au atoms are -2.37, -2.39 and -3.26 eV, respectively. Comparing with adsorption energies of Au_2 (-2.50 eV), Au_3 (-3.31 eV) and Au_4 (-2.67 eV), adsorption of atomic Au atoms is preferred same to stoichiometric surface. On hydrated surface, the adsorption energies of two Au atoms, three Au atoms and four Au atoms are -1.82, -3.50 and -3.03 eV, respectively. Comparing with adsorption energies of Au_2 (-2.44 eV), Au_3 (-2.89 eV) and Au_4 (-3.31 eV), respectively. It indicates that agglomeration of one more Au_n clusters is preferred on the hydrated surface.

On the stoichiometric B-termination, except single Au atom prefers to long bridge site of two surface O_1 sites, the most stable Au clusters adsorption configurations prefer Au atoms to surface octahedral iron atoms. On the reduced termination, one of the Au_n atoms prefers the adsorption site of the oxygen vacancy and other Au atoms prefer the surface iron atoms. On the hydrated termination, except single Au atom prefers to adsorb on bicoordinated O_1 site, for other Au clusters, one Au atom interacts directly with the formed surface hydroxyl group, and other Au atoms prefer the surface iron atoms. Comparing the single Au atom with H_2O adsorption on the

RSC Advances Accepted Manuscript

Fe_3O_4(001) B-termination, we found that H atom prefers to spillover on surface bicoordinated oxygen atom. It is to note that the most stable configurations of Au_n clusters differ on three surfaces. However, the adsorbed Au atoms to surface iron atoms have negative charge, and the Au atoms interacting either with surface oxygen atom or the formed surface hydroxyl have less negative or positive charge; and this trend is associated with their differences in electronegativity. It is also to note that charge transfer is stronger on the stoichiometric and reduced surface than on the hydrated surface, and hydration hinders the reduction of Au_n clusters on the surface.

In addition, we consider effect of the adsorbed Au_n clusters on oxidation state of the surface iron atoms in three surfaces. It is well known that the difference in total occupancy between Fe^{2+} and Fe^{3+} are amall (0.2-0.4 e),[40] so we calculated the magnetic moments of the three surfaces and surfaces with single Au adsorption (Fig.4). As we know, Au atom has $5d^{10}6s^1$ and 0.99 μ_B in gas phase, the magnetism of single Au changes to 0.09, 0.16 and 0.07 μ_B after adsorption on the three surfaces, respectively. This is mainly results by the single Au atom oxidized or reduced by surfaces and lost 0.418 e, -0.429 e and 0.429 e (Fig.3a). On the stoichiometric Fe_3O_4(001) surface (Fig.4a), we can clearly see that the magnetic moment of two octahedral iron atoms under the adsorbed Au atom changed from both 4.09 μ_B to 3.74 and 3.66 μ_B. It indicates that the oxidation state of two octahedral iron atoms changed from Fe^{3+} to Fe^{2+}. On the reduced Fe_3O_4(001) surface (Fig.4b), the magnetic moments of three octahedral iron atoms around oxygen vacancy are 3.61, 3.61 and 3.66 μ_B, respectively. The magnetic moment of one surface octahedral iron around oxygen vacancy changed from 3.61 to 4.07 μ_B after single Au atom adsorption. On the hydrated surface (Fig.4c), the magnetic moment of surface iron atom under hydroxyl is 4.11 μ_B. The magnetic moment of surface iron atom under hydroxyl changed from 4.11 to 3.69 μ_B after single Au atom adsorption. It indicates that the oxidation state of surface iron atoms can change after Au_n clusters adsorption.

RSC Advances Accepted Manuscript

(Fig. 4)

On the role of Au nanoparticles supported on iron oxides as active catalysts, the oxidation states of such nanoparticles have been discussed. It is found experimentally that positively charged Au atoms might have important implications in catalysis.[66] For single Au atom adsorption on the six terminations of the $Fe_3O_4(111)$ surface it is found that the adsorbed Au atom on the iron terminated surfaces is reduced and has negative charge, and while it is oxidized and has positive charge on the oxygen terminated surfaces.[29] On the $Fe_3O_4(001)$ surfaces it also shows that Au atoms on surface iron are reduced and have negative charge. Since either the reduction or oxidation of Au atoms on the surfaces depends on their relative electronegativities, oxygen terminated or oxygen rich surfaces are needed to oxidize the adsorbed Au atoms on the surface to bear positive charges. Another reason for having such positively charged Au atoms is the frontier orbital nature of CO and H_2 molecule, which need unsaturated sites from Au atoms for coordination.

Compared to stoichiometric surface, the surface hydroxyls can stabilize the Au_n on the hydrated surface as indicated by the calculated adsorption energies on both surfaces, and this is in agreement with the reported experiments.[17] For Au_n adsorption on the hydrated $Fe_3O_4(001)$ surface, one of the gold atoms interacts with the oxygen atom of hydroxyl groups. In addition, surface hydroxyls stabilizing Au_n clusters and enhancing the catalytic activities has also been found in other systems; e.g.; Au/MgO,[24-26] Au/SiO_2,[67] Au/FeO_x,[68] and Au/TiO_2. [23,27,69]

4. Conclusion

Since iron oxide supported gold nanoparticles have been found to have pronounced and promising catalytic activities in many reactions, we have computed the electronic structure and stability of gold clusters (Au_n, n = 1-4) adsorbed on the $Fe_3O_4(001)$ B-termination on the basis of the spin-polarized density functional theory by including the strong on-site Coulomb corrections

RSC Advances Accepted Manuscript

(GGA+U). It is found that the surface oxygen vacancy has lower formation energy than the surface iron vacancy; and the most stable hydrated surface has heterolytically dissociated H_2O and therefore surface hydroxyls, in agreement with the recent experimental studies.

On the clean and hydrated surfaces, single Au atom bonds to surface oxygen atoms, while larger Au clusters prefer to bond with surface iron atoms, while on the reduced termination, one of the Au_n atoms prefers the oxygen vacancy site and other Au atoms prefer surface iron atoms. It is found that the most stable configurations of Au_n clusters differ on three surfaces, and the adsorbed Au atoms to surface iron atoms have negative charge, and the Au atoms interacting either with surface oxygen atom or the formed surface hydroxyls have less negative or positive charge, in line with their differences in electronegativity. It is also to note that both stoichiometric and reduced surfaces have stronger charge transfer than the hydrated surface.

Apart from the different stable adsorption configurations, the adsorbed Au_n clusters also have different adsorption energies. Au_1 has the strongest adsorption on the stoichiometric surface; Au_2 and Au_3 have the strongest adsorption on the reduced surface, while Au_4 has the strongest adsorption on the hydrated surface. From Au_2 to Au_4 clusters, the clean surface has the lowest adsorption. As observed experimentally the hydrated surface can stabilize the Au_n clusters via the surface Au-OH interaction.

On the basis of the experimentally observed electronic structures of gold clusters, which are oxidized and have positive charge, and on our results that Au atoms have positive charge by interacting with surface oxygen atoms and negative charge by binding to surface iron atoms; it is to propose that oxygen terminated or oxygen rich surfaces are needed to oxidize gold cluster to bear positive charge for CO or H_2 coordination and activation.

Acknowledgments: This work was supported by the National Natural Science Foundation of China (No. 21073218), the National Basic Research Program of China (No. 2011CB201406),

RSC Advances Accepted Manuscript

Chinese Academy of Science and Synfuels China. Co., Ltd.

RSC Advances Accepted Manuscript

Fig. 1. Side (a) and top (b) views of Fe_3O_4(001) B-termination with possible adsorption sites (red ball for oxygen atom; blue ball for iron atom; small white ball for hydrogen atom; Sur represent surface, Sub represent subsurface)

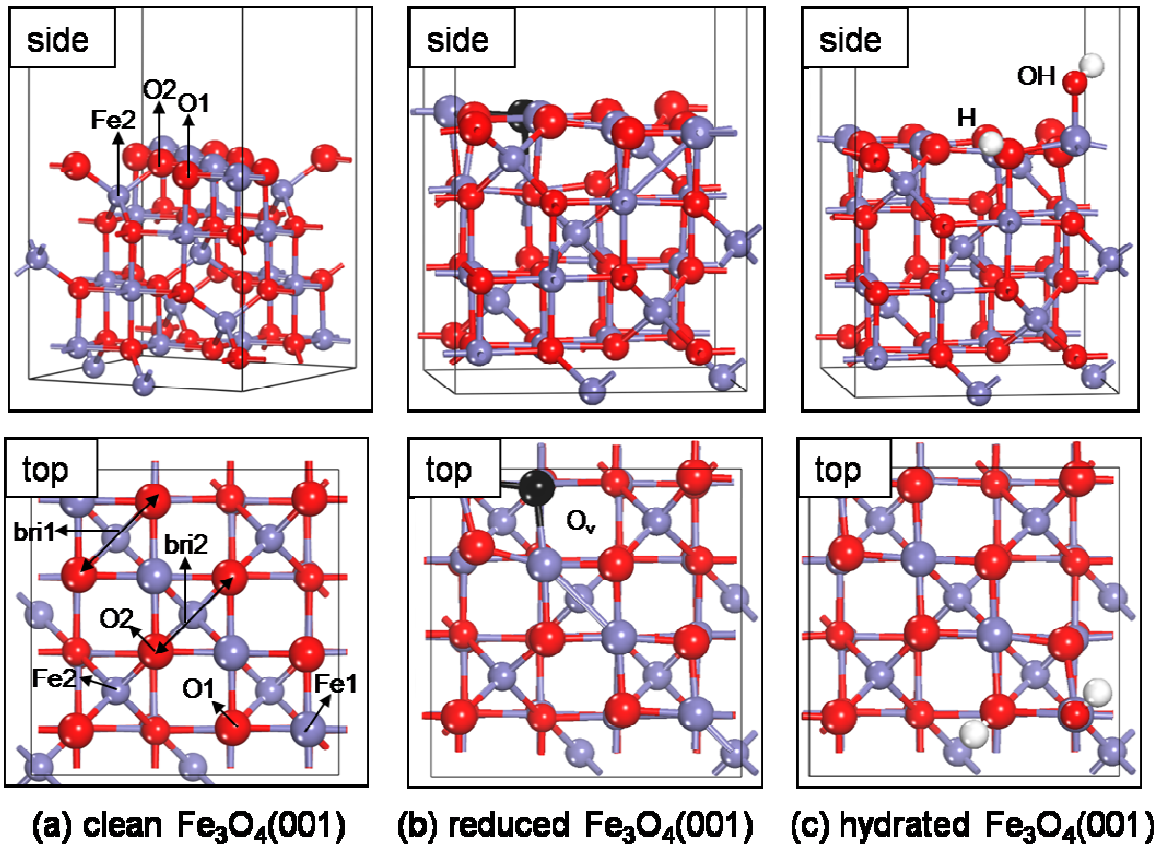

RSC Advances Accepted Manuscript

Fig. 2. Gas phase structures of Au_n clusters (n=1-4)

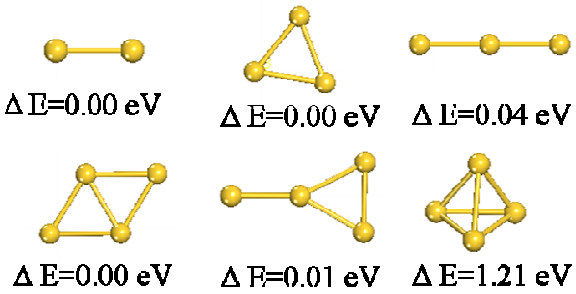

RSC Advances Accepted Manuscript

Fig. 3. Most stable Au_n adsorption configurations on the Fe_3O_4(001) B-termination [(A) stoichiometric surface; (B) reduced surface; (C) hydrated surface] with adsorption energies (eV), Au-Fe distances (Å), and the Bader charge of Au atoms (in parenthesis) (red ball for oxygen atom; blue ball for iron atom; white ball for hydrogen atom and yellow ball for gold atom)

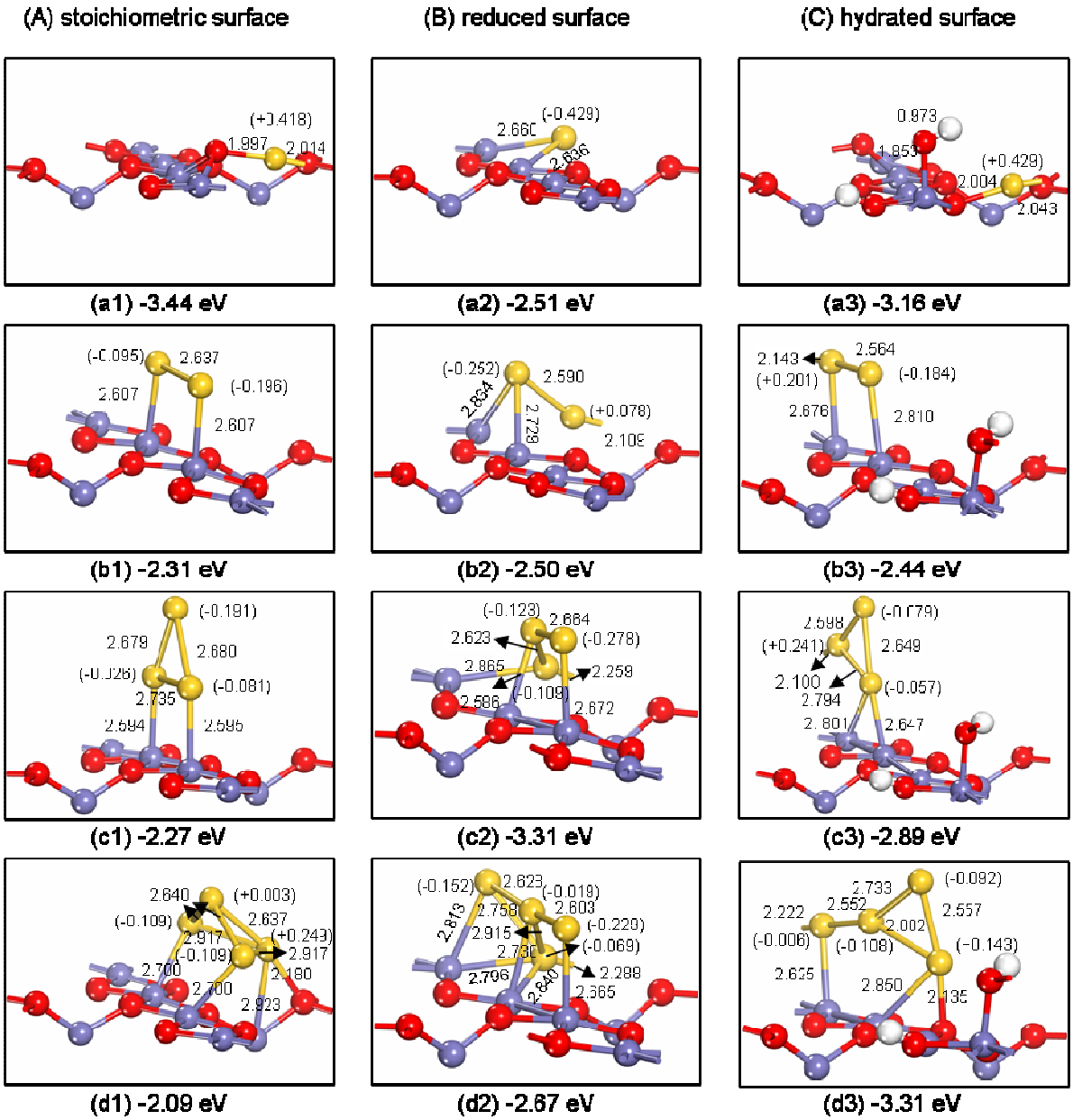

RSC Advances Accepted Manuscript

Fig. 4. Side views of the magnetic moment (μ_B) for three surfaces and single Au adsorption. (red ball for oxygen atom; blue ball for iron atom; white ball for hydrogen atom and yellow ball for gold atom)

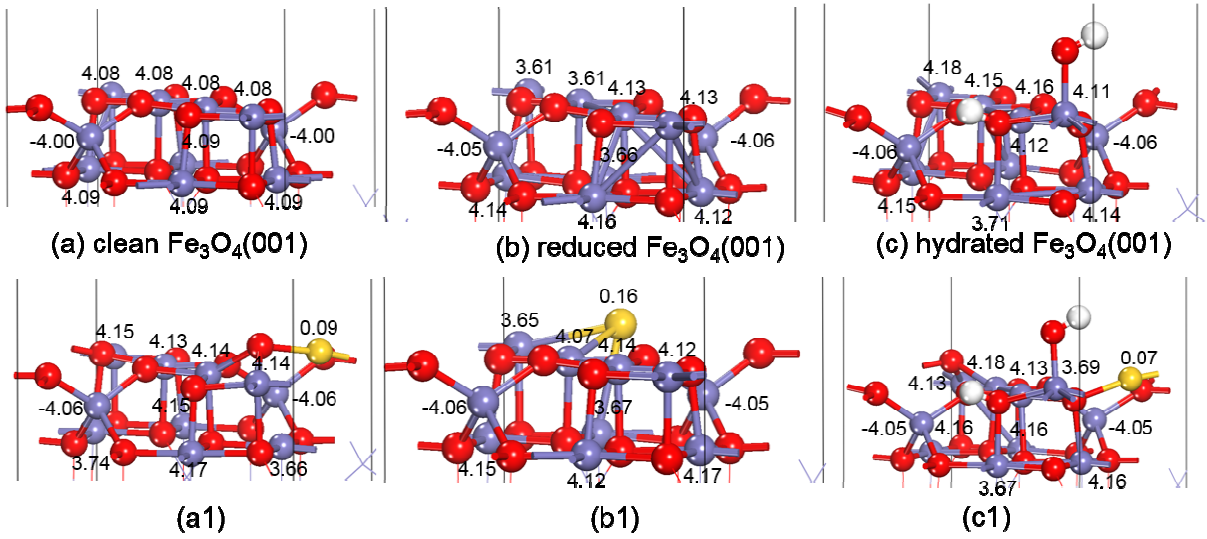

RSC Advances Accepted Manuscript

References

1 M. Haruta, *Gold. Bull.*, 2004, **37**, 27-36.

2 R. Meyer, C. Lemire, S. Shaikhutdinov and H. Freund, *Gold. Bull.*, 2004, **37**, 72-124.

3 A. S. K. Hashmi and G. J. Hutchings, *Angew. Chem. Int. Edit.*, 2006, **45**, 7896-7936.

4 B. K. Min and C. M. Friend, *Chem. Rev.*, 2007, **107**, 2709-2724.

5 C. Ratnasamy and J. Wagner, *Catal. Rev.*, 2009, **51**, 325-440.

6 G. Bond, *Gold. Bull.*, 2009, **42**, 337-342.

7 B. Hammer and J. Norskov, *Nature*, 1995, **376**, 238-240.

8 M. Chen and D. W. Goodman, *Chem. Soc. Rev.*, 2008, **37**, 1860-1870.

9 M. S. Chen and D. W. Goodman, *Science*, 2004, **306**, 252-255.

10 A. A. Herzing, C. J. Kiely, A. F. Carley, P. Landon and G. J. Hutchings, *Science*, 2008, **321**, 1331-1335.

11 L. Giordano, G. Pacchioni, J. Goniakowski, N. Nilius, E. Rienks and H. Freund, *Phys. Rev. Lett.*, 2008, **101**, 26102.

12 K. T. Rim, D. Eom, L. Liu, E. Stolyarova, J. M. Raitano, S.-W. Chan, M. Flytzani-Stephanopoulos and G. W. Flynn, *J. Phys. Chem. C*, 2009, **113**, 10198-10205.

13 Y. Lee, M. A. Garcia, N. A. F. Huls and S. Sun, *Angew. Chem. Int. Edit.*, 2010, **49**, 1271-1274.

14 L. Allard, A. Borisevich, W. Deng, R. Si, M. Flytzani-Stephanopoulos and S. Overbury, *J. Electron Microsc.*, 2009, **58**, 199–212.

15 W. Deng, C. Carpenter, N. Yi and M. Flytzani-Stephanopoulos, *Top. Catal.*, 2007, **44**, 199-208.

RSC Advances Accepted Manuscript

16 S. Shaikhutdinov, R. Meyer, M. Naschitzki, M. Bäumer and H. Freund, *Catal. Lett.*, 2003, **86**, 211-219.

17 Y. Zhu, L. Tian, Z. Jiang, Y. Pei, S. Xie, M. Qiao and K. Fan, *J. Catal.*, 2011, **281**, 106-118.

18 N. Spiridis, R. P. Socha, B. Handke, J. Haber, M. Szczepanik and J. Korecki, *Catal. Today*, 2011, **169**, 24-28.

19 K. Jordan, S. Murphy and I. V. Shvets, *Surf. Sci.*, 2006, **600**, 5150-5157.

20 C. Gatel and E. Snoeck, *Surf. Sci.*, 2006, **600**, 2650-2662.

21 C. Gatel and E. Snoeck, *Surf. Sci.*, 2007, **601**, 1031-1039.

22 Z. Novotný, G. Argentero, Z. Wang, M. Schmid, U. Diebold and G. S. Parkinson, *Phys. Rev. Lett.*, 2012, **108**, 216103.

23 G. M. Veith, A. R. Lupini, S. J. Pennycook and N. J. Dudney, *ChemCatChem*, 2010, **2**, 281-286.

24 M. A. Brown, E. Carrasco, M. Sterrer and H.-J. Freund, *J. Am. Chem. Soc.*, 2010, **132**, 4064-4065.

25 M. A. Brown, Y. Fujimori, F. Ringleb, X. Shao, F. Stavale, N. Nilius, M. Sterrer and H.-J. Freund, *J. Am. Chem. Soc.*, 2011, **133**, 10668-10676.

26 D.-e. Jiang, S. H. Overbury and S. Dai, *J. Phys. Chem. Lett.*, 2011, **2**, 1211-1215.

27 P. Ganesh, P. R. C. Kent and G. M. Veith, *J. Phys. Chem. Lett.*, 2011, **2**, 2918-2924.

28 T. Yang, X.-D. Wen, Y.-W. Li, J. Wang and H. Jiao, *Surf. Sci.*, 2009, **603**, 78-83.

29 X. Yu, S.-G. Wang, Y.-W. Li, J. Wang and H. Jiao, *J. Phys. Chem. C*, 2012, **116**, 10632-10638.

30 X. Yu, X. Tian and S. Wang, *Surf. Sci.*, 2014, **628**, 141-147.

31 A. Kiejna, T. Ossowski and T. Pabisiak, *Phys. Rev. B*, 2012, **85**, 125414.

RSC Advances Accepted Manuscript

32 P. E. Blöchl, *Phys. Rev. B*, 1994, **50**, 17953-17979.

33 G. Kresse and D. Joubert, *Phys. Rev. B*, 1999, **59**, 1758-1775.

34 G. Kresse and J. Furthmüller, *Phys. Rev. B*, 1996, **54**, 11169-11186.

35 G. Kresse and J. Hafner, *Phys. Rev. B*, 1994, **49**, 14251-14269.

36 J. P. Perdew, K. Burke and M. Ernzerhof, *Phys. Rev. Lett.*, 1996, **77**, 3865-3868.

37 V. Anisimov, F. Aryasetiawan and A. Lichtenstein, *J. Phys.: Condens. Matter*, 1997, **9**, 767-808.

38 V. Anisimov, I. S. Elfimov, N. Hamada and K. Terakura, *Phys. Rev. B*, 1996, **54**, 4387-4390.

39 H. P. Pinto and S. D. Elliott, *J. Phys.: Condens. Matter*, 2006, **18**, 10427-10436.

40 X. Yu, Y. Li, Y.-W. Li, J. Wang and H. Jiao, *J. Phys. Chem. C*, 2013, **117**, 7648-7655.

41 X. Yu, C.-F. Huo, Y.-W. Li, J. Wang and H. Jiao, *Surf. Sci.*, 2012, **606**, 872-879.

42 L. Finger, R. Hazen and A. Hofmeister, *Phys. Chem. Miner.*, 1986, **13**, 215-220.

43 H. Okudera, K. Kihara and T. Matsumoto, *Acta Crystallogr. B*, 1996, **52**, 450-457.

44 H. J. Monkhorst and J. D. Pack, *Phys. Rev. B*, 1976, **13**, 5188-5192.

45 S. Ju, T.-Y. Cai, H.-S. Lu and C.-D. Gong, *J. Am. Chem. Soc.*, 2012, **134**, 13780-13786.

46 G. J. Martin, R. S. Cutting, D. J. Vaughan and M. C. Warren, *Am. Mineral.*, 2009, **94**, 1341-1350.

47 R. Pentcheva, F. Wendler, H. L. Meyerheim, W. Moritz, N. Jedrecy and M. Scheffler, *Phys. Rev. Lett.*, 2005, **94**, 126101.

48 R. Pentcheva, W. Moritz, J. Rundgren, S. Frank, D. Schrupp and M. Scheffler, *Surf. Sci.*, 2008, **602**, 1299-1305.

49 M. Fonin, R. Pentcheva, Y. S. Dedkov, M. Sperlich, D. V. Vyalikh, M. Scheffler, U. Rudiger and G. Guntherodt, *Phys. Rev. B*, 2005, **72**, 104436.

RSC Advances Accepted Manuscript

50 Z. Lodziana, *Phys. Rev. Lett.*, 2007, **99**, 206402.

51 C. Zhang, A. Michaelides, D. A. King and S. J. Jenkins, *J. Am. Chem. Soc.*, 2010, **132**, 2175-2182.

52 H. Häkkinen and U. Landman, *Phys. Rev. B*, 2000, **62**, R2287-R2290.

53 X.-B. Li, H.-Y. Wang, X.-D. Yang, Z.-H. Zhu and Y.-J. Tang, *J. Chem. Phys.*, 2007, **126**, 084505.

54 J. Zhao, J. Yang and J. G. Hou, *Phys. Rev. B*, 2003, **67**, 085404.

55 J. C. Idrobo, W. Walkosz, S. F. Yip, S. Öğüt, J. Wang and J. Jellinek, *Phys. Rev. B*, 2007, **76**, 205422.

56 J. Wang, G. Wang and J. Zhao, *Phys. Rev. B*, 2002, **66**, 035418.

57 P. K. Jain, *Struct. Chem.*, 2005, **16**, 421-426.

58 F. Baletto and R. Ferrando, *Rev. Mod. Phys.*, 2005, **77**, 371-423.

59 B. Assadollahzadeh and P. Schwerdtfeger, *J. Chem. Phys.*, 2009, **131**, 064306.

60 W. Mason *American Institute of Physics Handbook*; McGraw-Hill: New York, 1972.

61 L. C. Allen, *J. Am. Chem. Soc.*, 1989, **111**, 9003-9014.

62 Z. Yang, T. K. Woo, M. Baudin and K. Hermansson, *J. Chem. Phys.*, 2004, **120**, 7741-7749.

63 M. Nolan and S. Elliott, *Phys. Chem. Chem. Phys.*, 2006, **8**, 5350-5358.

64 N. Mulakaluri, R. Pentcheva and M. Scheffler, *J. Phys. Chem. C*, 2010, **114**, 11148-11156.

65 G. S. Parkinson, Z. k. Novotný, P. Jacobson, M. Schmid and U. Diebold, *J. Am. Chem. Soc.*, 2011, **133**, 12650-12655.

66 J. C. Fierro-Gonzalez and B. C. Gates, *Chem. Soc. Rev.*, 2008, **37**, 2127-2134.

67 K. Qian, W. Zhang, H. Sun, J. Fang, B. He, Y. Ma, Z. Jiang, S. Wei, J. Yang and W. Huang, *J. Catal.*, 2011, **277**, 95-103.

RSC Advances Accepted Manuscript

68 K. Zhao, B. Qiao, J. Wang, Y. Zhang and T. Zhang, *Chem. Commun.*, 2011, **47**, 1779–1781.

69 J. K. Edwards, E. Ntainjua N, A. F. Carley, A. A. Herzing, C. J. Kiely and G. J. Hutchings, *Angew. Chem. Int. Edit.*, 2009, **48**, 8512-8515.

RSC Advances Accepted Manuscript